



Robust Harmonic Elimination Method for Various Load Conditions

Zakaria Reguieg^{a,*}, Ismail Bouyakoub^a, Fayçal Mehedi^a, Fatiha Bouhadji^a

^a *Laboratoire Génie Electrique et Energies Renouvelables (LGEER), Hassiba Benbouali University of Chlef, Faculty of Technology, Chlef, Algeria.*

ARTICLE INFO

Article history:

Received September 30, 2024

Accepted October 22, 2024

Keywords:

Photovoltaic,
Shunt active power filter,
Harmonic currents,
Direct power control.

ABSTRACT

The present study implements a Direct Power Control (DPC) strategy to manage a photovoltaic (PV) system functioning as a shunt active power filter (shunt APF), aimed at providing reactive power compensation and mitigating harmonic currents while nonlinear loads are present. The DPC identification method effectively detects harmonics generated by these loads, while the shunt APF utilizes a maximum power point tracking perturb and observe (PO-MPPT) technique to optimize energy extraction via the PV source. Through extensive simulations in MATLAB Simulink, the research demonstrates the robustness of the shunt APF in eliminating harmonics under various load conditions, highlighting its potential for enhancing power quality (PQ) in electrical grids.

1. INTRODUCTION

As the world confronts the urgent demand for sustainable energy solutions, photovoltaic (PV) systems have arisen as a promising option, providing a clean and renewable substitute for conventional fossil fuels (Allouhi et al., 2023; Obaideen et al., 2023). Nonetheless, the incorporation of these systems into current power grids brings forth distinctive challenges, notably harmonic distortions and the necessity for reactive power compensation (Rajesh Garikapati et al., 2023). In traditional practice, shunt active power filters (shunt APF) have been utilized to address these issues (Boopathi & Indragandhi, 2023; Dash & Sadhu, 2023).

Harmonics present a significant challenge in electrical systems, often leading to various operational issues and inefficiencies. These issues include increased losses in power distribution systems, overheating of equipment, and distortion of voltage and current waveforms (Reguieg, Bouyakoub, Mehedi, et al., 2024a). Additionally, harmonics can interfere with sensitive electronic equipment, causing malfunctions and reducing their lifespan. Moreover, harmonics can result in poor power quality

* Corresponding author, E-mail address: z.reguieg@univ-chlef.dz

Tel : + 213 541126997



(PQ), leading to voltage fluctuations, flickering lights, and disruptions in power supply. Overall, mitigating harmonics is essential for ensuring the efficiency, reliability, and safety of electrical systems (Bajaj & Singh, 2020; Taghvaie et al., 2023).

Furthermore, there is a growing emphasis on PQ enhancement through the utilization of active filters and devices (Lumbreras et al., 2020; Reguieg, Bouyakoub, Mehedi, et al., 2024b). Incorporating PV systems into active filters has emerged as a viable approach for improving PQ. Among various active filter converter types, shunt APF is notable for their demonstrated effectiveness in mitigating harmonics, correcting power factor, and balancing reactive power (Freitas et al., 2023; Sahoo et al., 2023). Shunt APF uses two-level inverter technology to reduce harmonic distortions and provide reactive power compensation in electrical systems, especially for medium power range applications with non-linear loads. This technique is useful due to semiconductor device limitations in handling higher power levels (Imam et al., 2020). The reference waveform for compensatory current in a shunt APF can be calculated using various methodologies. One method is indirect measurement, monitoring voltage across the capacitor. Other methods include direct harmonic analysis or model predictive control strategies to optimize the waveform, ensuring effective performance and improving PQ (Szromba, 2023).

The study explores the combined use of a shunt APF with a grid-connected PV system to improve PQ and operational efficiency. This integration reduces costs, improves system efficiency, and contributes to a sustainable electrical grid. Direct power control (DPC) techniques is used in the study to optimize the PV system's power injection into the grid, promoting renewable energy utilization and transitioning to greener energy solutions.

The objectives of this paper are:

- Apply the DPC algorithm to a shunt APF that is connected to PV panel Maximum Power Point Tracking via Perturb and Observe (PO-MPPT).
- Reduce harmonics generated by nonlinear loads (NLs).
- Conduct robust testing of the DC bus under varying load conditions and a variety of types of loads to evaluate the reliability and practicality of the integrated system.

Figure (1) illustrates a renewable energy system with a power source, PV system, NLs, and shunt APF. The PV system comprises a boost converter with MPPT technique for optimal energy extraction. The shunt APF uses the DPC algorithm with harmonic identification to reduce distortions and ensure harmonious operation at the point of common coupling.

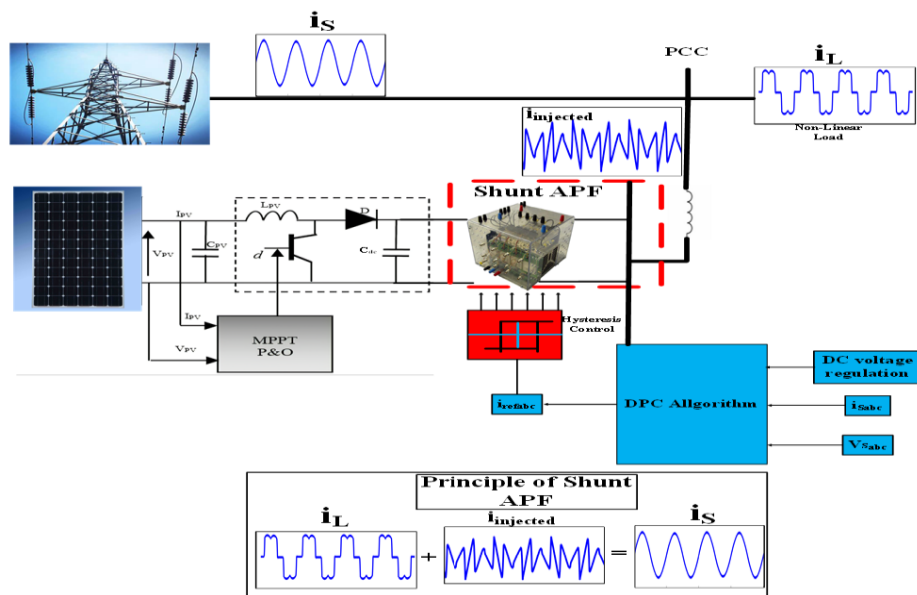


Fig 1. Proposed system configuration

2. PRINCIPLES OF OPERATIONS FOR THE SUGGESTED DPC STRATEGY ON PV-CONNECTED SHUNT APF

2.1 Principles of DPC

The DPC technique utilized in this study is adapted from the direct torque control (DTC) approaches employed in electric motor drives (Djazia & Sarra, 2023; Sen et al., 2023). In DPC, the reactive and active powers function similarly to torque and flux amplitude in DTC, this nonlinear control method enables direct selection of the suitable voltage vector, eliminating the need for modulation techniques or coordinate transformations (Shi & Jin, 2023).

The core principle of DPC involves the real-time selection of optimal switching states from a predefined table, which is correspondingly to the current location of the source voltage vector and the calculated deviations in reactive and active power. This approach allows for immediate adjustments to the inverter's output, enhancing the system's adaptability to changing load conditions. Additionally, the integration of an anti-windup fractional-order proportional-integral-derivative (PID) controller within a continuous regulation loop ensures that the DC bus voltage stays at a specified reference level, thereby improving stability and the reliability of the overall power system (Essoussi et al., 2023).

The proposed system calculates reactive and active powers in real-time using measured source voltages and currents for efficient power control. The reactive power reference is in the zero set, guaranteeing the power factor operation's unity, making certain all power is used without any reactive component. The active power reference is determined by multiplying peak source current with optimal voltage output from the PV generator, optimizing energy extraction from solar panels while maintaining system stability (Rath & Srungavarapu, 2023). Hysteresis regulators process active and reactive power errors to limit them within defined thresholds, ensuring stable inverter operation. The outputs and the location of the source voltage vector go into a switching table to determine the appropriate inverter switching states (Sen et al., 2023). This switching table, outlined in table 1, represents the DPC strategy, facilitating the best inverter switching states to select based on the given inputs. Instantaneous reactive and active powers are calculated using the following equations:

$$P_s = V_{sa}I_{sa} + V_{sb}I_{sb} + V_{sc}I_{sc} \tag{1}$$

$$Q_s = \frac{1}{\sqrt{3}}[(V_{sb} - V_{sc})I_{sa} + (V_{sa} - V_{sa})I_{sb} + (V_{sa} - V_{sa})I_{sc}] \tag{2}$$

$$S_s = P_s + jQ_s \tag{3}$$

Table 1. DPC strategy switching

C_p	C_q	State 1	State 2	State 3	State 4	State 5	State 6	State 7	State 8	State 9	State 10	State 11	State 12
1	1	Y.6	Y.7	Y.1	Y.0	Y.2	Y.7	Y.3	Y.0	Y.4	Y.7	Y.5	Y.0
1	0	Y.7	Y.7	Y.0	Y.0	Y.7	Y.7	Y.0	Y.0	Y.7	Y.7	Y.0	Y.0
0	1	Y.6	Y.1	Y.1	Y.2	Y.2	Y.3	Y.3	Y.4	Y.4	Y.5	Y.5	Y.6
0	0	Y.1	Y.2	Y.2	Y.3	Y.3	Y.4	Y.4	Y.5	Y.5	Y.6	Y.6	Y.1

The inverter output voltage reference vector is determined by the acceptable levels of reactive and active power, which necessitates identifying the sector corresponding to the angle in the stationary (α, β) reference frame among the reference vector and the α -axis. This angle is calculated utilizing an inverse function of trigonometry applied to the voltage vector components, allowing for the determination of

the sector number. Once this sector number is established, the appropriate inverter output voltage vector is chosen using a preset switching table, ensuring that the system can effectively respond to the reactive and active power demands as indicated by the hysteresis regulators (Boudechiche et al., 2021; Essoussi et al., 2023).

$$\theta_p = \tan^{-1}\left(\frac{V_{s\beta}}{V_{s\alpha}}\right) \quad (4)$$

2.1.1 Adjusting the DC connection

The PI controller is accustomed to maintaining a stable DC bus voltage near its value of reference. Based on the inaccuracy, the control output is improved to reflect the error between the recent DC bus voltage and the intended reference, improving steady-state accuracy. The anti-windup mechanism prevents excessive integral term accumulation during saturation conditions, ensuring responsiveness and voltage regulation without instability or overshoot, as demonstrated in Fig. (2).

The connection among the voltage of the DC link (V_{dc}) as well as the reference value (V_{dc-ref}) can be expressed as a second-order transfer function:

$$\frac{V_{dc}}{V_{dc-ref}} = \frac{K_p * K_i / C}{S^2 + (K_p / C)S + K_p K_i / C} \quad (5)$$

$$\frac{V_{dc}}{V_{dc-ref}} = \frac{w_n^2}{S^2 + 2\varepsilon w_n S + w_n^2} \quad (6)$$

With s is the complex frequency variable, ε is the damping ratio and w_n is the natural frequency.

The PI controller plays a critical role in regulating the active power reference (P^*) by continuously monitoring the discrepancy among the actual DC link voltage (V_{dc}) as well as the desired reference value (V_{dc-ref}). This ensures that the DC bus remains charged at the desired voltage level for proper operation of the active power filter and injection of available PV power. Fig. (2) illustrates the DPC algorithm utilized in the proposed system (Rath & Srungavarapu, 2023).

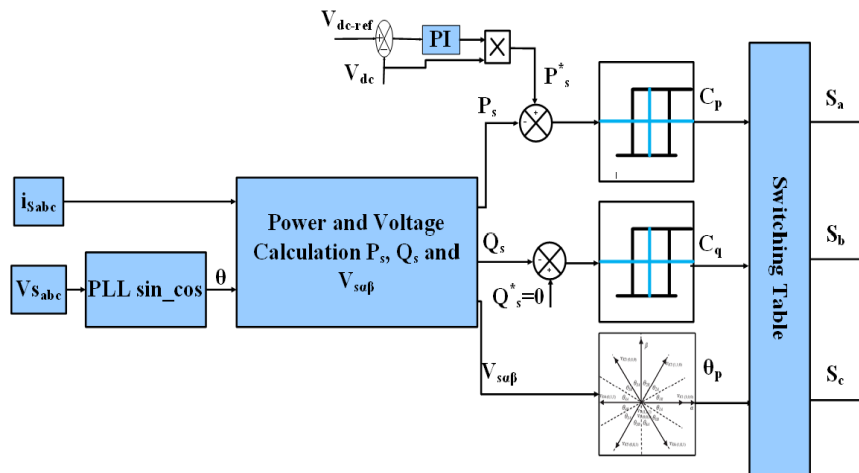


Fig 2. DPC algorithm

2.1 PV system modelling

In order to simulate the PV panel, the single-diode equivalent circuit is adopted. This circuit shows the PV cell as a source of current in parallel with a diode, like what Fig. (3) depicts.

The typical equation for current-voltage (I-V) for the PV cell can be expressed as:

$$V_{PV} = V_{do} - R_S I_{Pv} \tag{7}$$

$$I_{PV} = I_{Pv} - I_0 \left[\exp\left(\frac{q}{nKT} V_{do}\right) - 1 \right] - \left(V_{do} \frac{V_{PV} + R_S I_{PV}}{R_{Sh}} \right) \tag{8}$$

With I_{Pv} photocurrent, I_0 is the diode current, I_{sh} is the current through the shunt resistance (R_{sh}) and I_{Pv} is the current output within the PV cell.

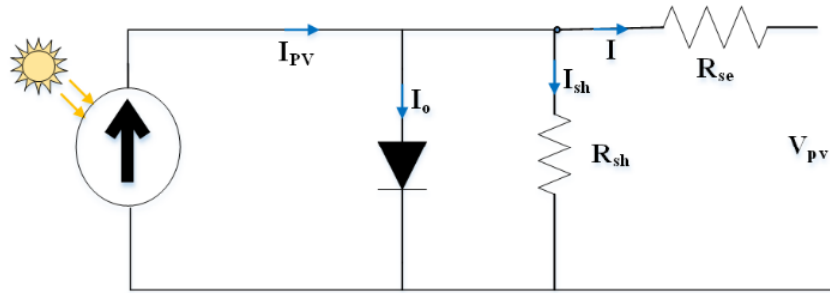


Fig 3. PV array modeling

2.3 Boost converter

Through the usage of a voltage source inverter, the boost converter facilitates the continuous transmission of electricity from a PV to the electrical grid. By controlling voltage and current levels, this configuration ensures stable electricity production, effective solar energy usage, and stability in the grid-connected solar power system (Debdouche et al., 2023). The boost converter's scheme is shown in Figure (4).

2.3.1 Command of the Boost Converter

The PV generator voltage is adjusted to meet a reference value defined by the P&O MPPT algorithm as part of the control strategy for the boost converter's current and voltage regulation. Considering the voltage's output controller and the adjustment of the PV current within the inner loop for current control, the current reference is calculated. To guarantee effective power conversion and grid integration, the boost converter's duty cycle (D) is calculated by taking the PV voltage, PV current, and output voltage compensations into account (Reguieg, Bouyakoub, & Mehedi, 2024).

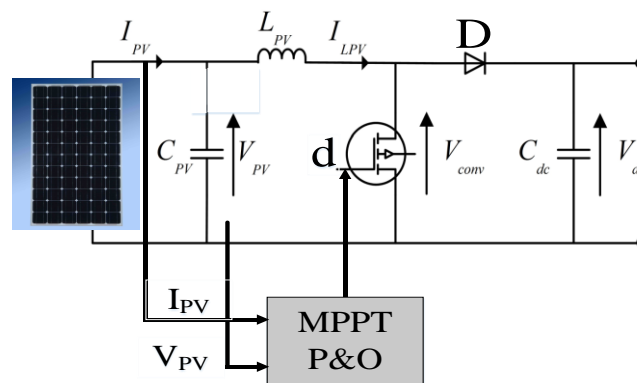


Fig 4. Boost converter with P&O MPPT

3. RESULTS OF SIMULATIONS

To assess the efficacy of the proposed technique, a series of simulation experiments were executed within the MATLAB/Simulink framework, which is widely utilized for modeling and simulating dynamic systems. The simulation parameters were configured to deliver a root mean square voltage of 231 V at a frequency of 50 Hz to a NL, specifically a rectifier (designated as PD3) that interfaces with an RL circuit, thereby allowing for the examination of how the system behaves under various load scenarios and the efficiency of the control strategies implemented. This setup facilitates the examination of PQ issues and how the system behaves dynamically, particularly within the framework of renewable energy integration and grid stability. The RL circuit parameters for the initial load are $R1 = 57 \Omega$ and $L1 = 20 \text{ mH}$, whereas the second load's, $R2 = 80 \Omega$ and $L2 = 20 \text{ mH}$. Additionally, a linear load with active power (P) = 500 W and reactive power (Q) = 100 VAR is incorporated. The PV cell operates under radiation of 1000 and a temperature of 25°C .

Three tests were performed, each involving different load conditions. Initially, the simulation was conducted with a NL alone. Subsequently, the second test involved varying parameters of the NL. In the third test, the load configuration initially consisted of both a NL and a linear load. Subsequently, the configuration was altered to include only the NL.

3.1 Case 1: Nonlinear Load

The load current, source current, and injected current by the shunt APF are shown in Figure (5). It displays that the shunt APF effectively injects current in order to make up for the harmonic components introduced by the NL, resulting in a balanced and nearly sinusoidal source current.

Figure (6) provides a thorough examination of the shunt APF's DC bus voltage, in addition to the source voltage and current. The DC bus voltage's consistency indicates how well the APF is regulating and control mechanisms, which are crucial for maintaining consistent operational performance with NLS present. This stability ensures that the APF can dynamically respond to fluctuations in load conditions while minimizing harmonic distortion in the source current, thereby enhancing overall PQ in the system.

Figure (7) illustrates the THD of the load current, quantified at 27.60%, which signifies a substantial existence of harmonic elements caused by the load's nonlinear properties. Conversely, the source current exhibits a significantly lower THD of 1.71%, indicating the effective execution of the shunt APF in mitigating distortion of harmonics and restoring the quality of the source current. This disparity in THD values underscores the APF's capability to enhance PQ by compensating for the harmonics introduced by the NL, thereby ensuring a more sinusoidal current waveform at the source.

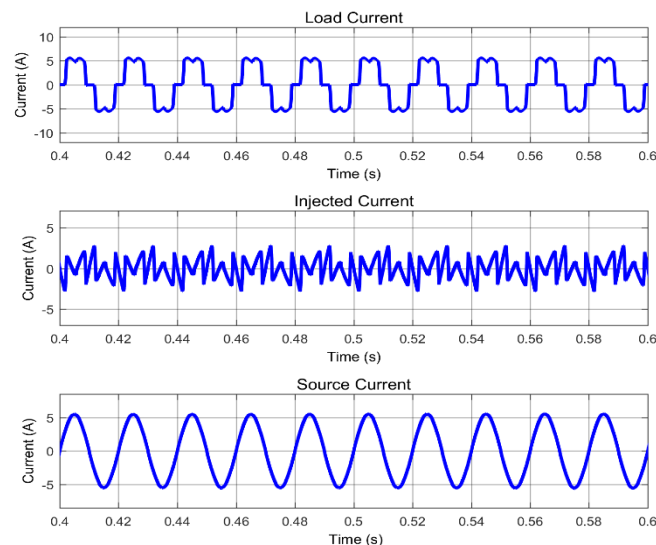


Fig 5. Load, shunt APF injected, and source currents analysis

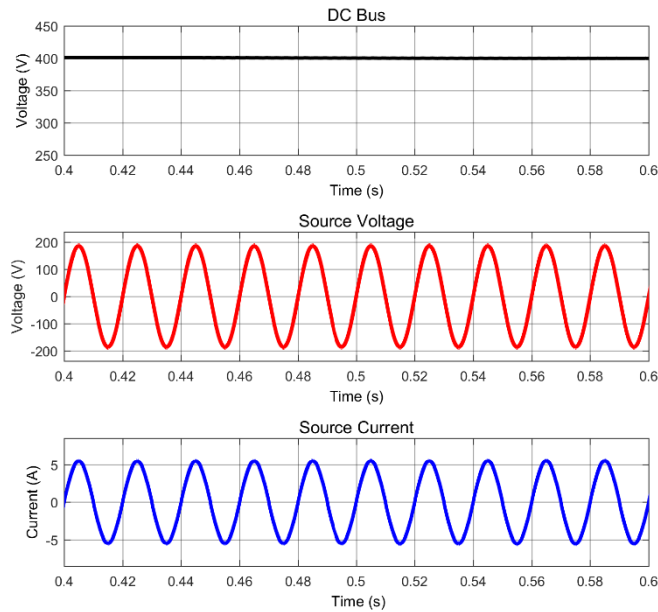


Fig 6. DC bus voltage, source voltage, and source current analysis

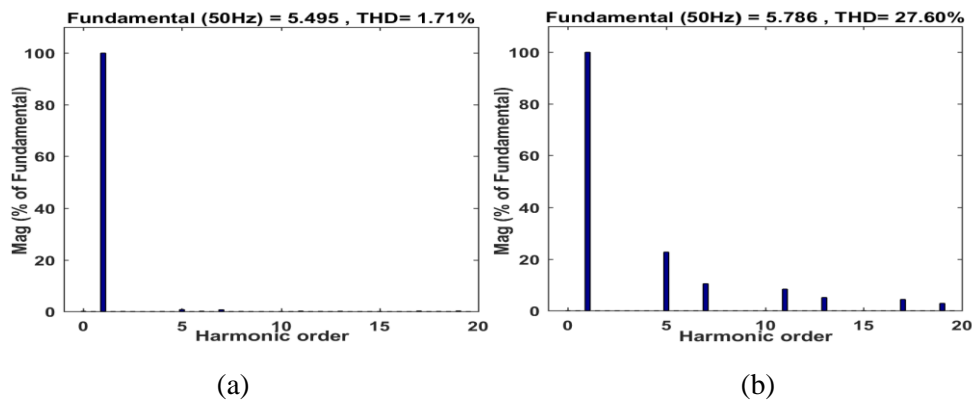


Fig 7. THD analysis: (a) source currents, (b) load current

3.2 Case 2: Nonlinear Load Variation

In case 2, Fig. (8) depicts the load current, injected current by the shunt APF, and the source current. At 0.7 seconds, a variation in the NL is applied, showcasing the adaptability of the filter to accommodate the change. The shunt APF promptly injects current to mitigate harmonics from the second NL.

Figure (9) illustrates the DC bus of the Shunt APF, demonstrating rejection of perturbation at 0.7 seconds and returning to the reference voltage of 400 V. Additionally, it displays the source current and source voltage.

Furthermore, Fig. (10) illustrates the THD of the second NL current, quantified at 28.12%, indicating a substantial presence of harmonic components due to the nonlinear characteristics of the load. In contrast, the source current exhibits a significantly lower THD of 1.86%, demonstrating the efficacy of the shunt APF in mitigating harmonic distortions introduced by the load.

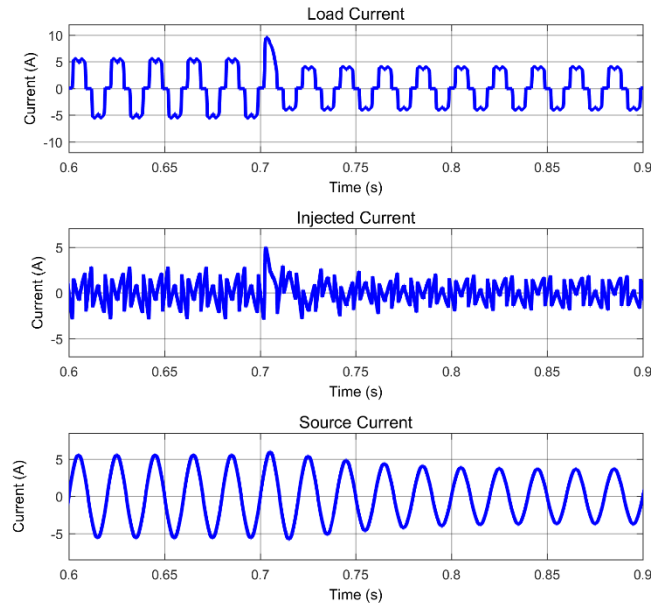


Fig 8. Analysis of load, shunt APF injected, and source currents during NL variation

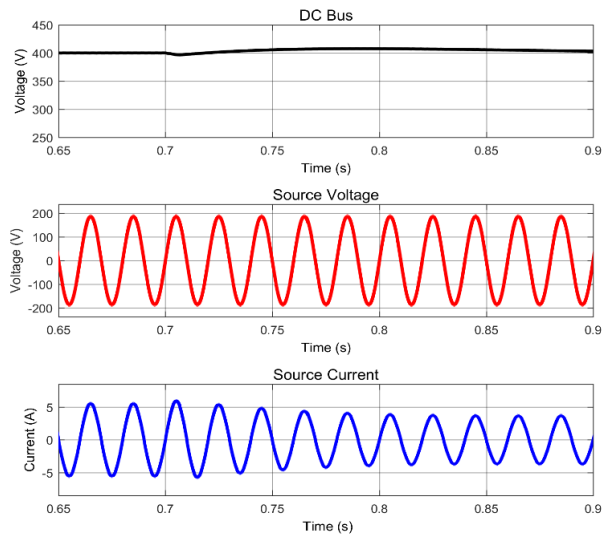


Fig 9. DC bus voltage, source voltage, and source current analysis during NL variation

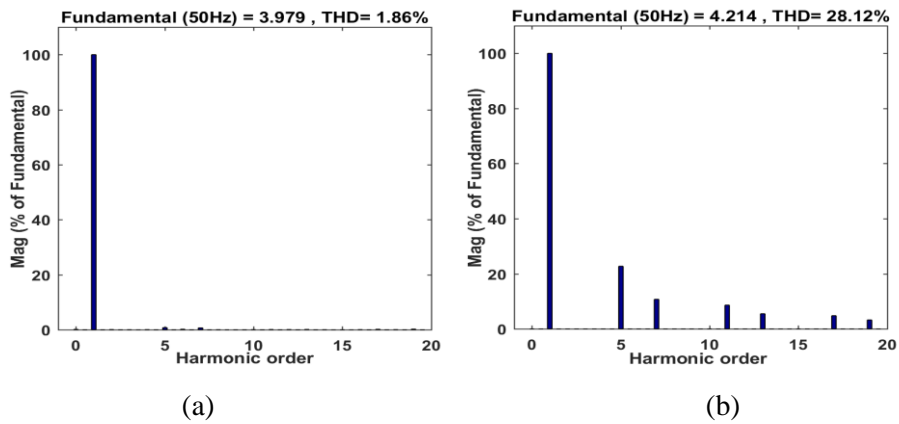


Fig 10. Second load THD analysis: (a) source currents, (b) load current

3.3 Case 3: Simulation Analysis of Linear Load Combined with NL, NL Variation

The load current of the linear load when combined with the NL is shown in Figure (11) between time spans of 0.6 and 0.7 seconds, followed by a variation to the NL at 0.7 seconds. The plot illustrates the injected current and the source current during this transformation.

The DC bus voltage is shown in Figure (12) while the 400V reference voltage is maintained. By 0.7 seconds, there is a rejection of perturbation, indicating stability in the system. Additionally, the plot shows the source voltage and source current throughout the simulation.

4. CONCLUSION

The PV-DPC Shunt APF method emerges as a promising solution for enhancing PQ. Through comprehensive simulation analyses, the method demonstrates its effectiveness and adaptability across various load conditions. Tests reveal the system's capability to mitigate harmonic distortions and ensure a balanced source current, even when subjected to load variations. Moreover, with different load configurations, the technique effectively maintains the source current's THD within the global IEEE limitations.

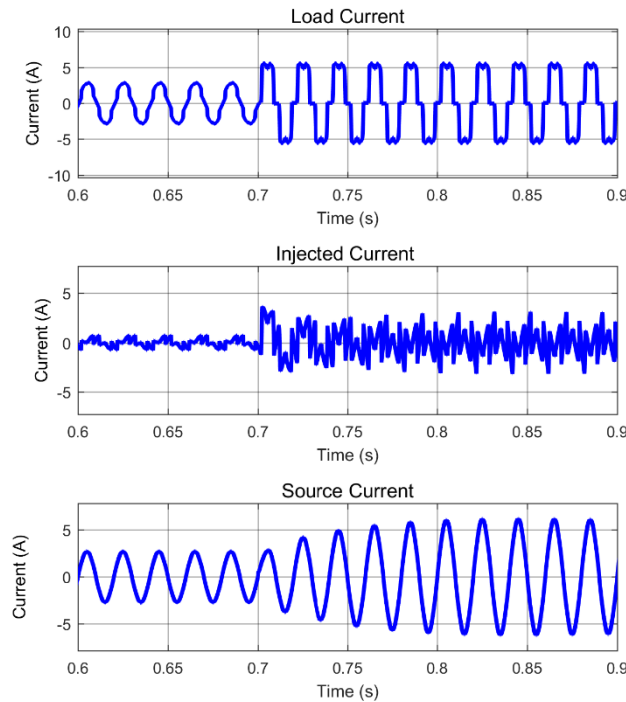


Fig 11. Analysis of load, shunt APF injected, and source currents during linear load with nonlinear load and variation to nonlinear load

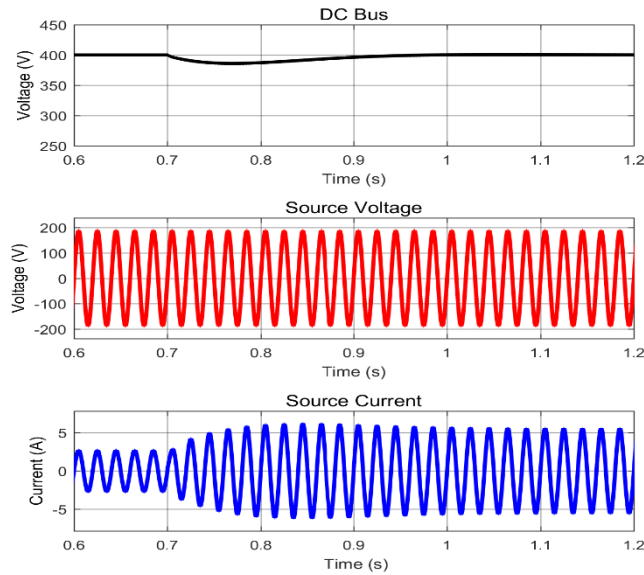


Fig 12. Analysis of the third case's DC bus voltage, source voltage and current

NOMENCLATURE

C	Capacitance of the DC-link (F)
C _p	Active power control signal
C _q	Reactive power control signal
I _o	Diode saturation current (A)
I _{ph}	Photocurrent (A)
I _{pv}	Current output of the PV cell (A)
I _{sa,Isb, Isc}	Phase currents of phases a, b and c (A)
j	Imaginary unit
k	Boltzmann constant (J/K)
K _{p, Ki}	Proportional and integral controller gains
n	Ideality factor of the diode
P _s	System's active power (w)
q	Elementary charge of an electron (C)
Q _s	System's Reactive power (VAR)
R _s	Series resistance of the PV cell (Ω)
R _{sh}	Shunt resistance (Ω)
S _s	Apparent power of the system (VA)
State 1, State 2, ..., State 12	Switching states representing specific control angles in the converter's operation.
T	Temperature in Kelvin (K)
V _{dc}	DC-link voltage (V)
V _{dc-ref}	Reference DC-link voltage (V)
V _{do}	Diode voltage (V)
V _{pv}	Output voltage of the PV cell (V)
V _{sa, Vsb, Vsc}	Phase voltages of phases a,b and c (V)
ω _n	Natural frequency (rad/s)
Y.1, Y.2, ..., Y.12	Voltage space vectors representing switching combinations in the converter.
ε	Damping ratio

REFERENCES

- Allouhi, A., Rehman, S., Buker, M. S., & Said, Z. (2023). Recent technical approaches for improving energy efficiency and sustainability of PV and PV-T systems: A comprehensive review. *Sustainable Energy Technologies and Assessments*, 56(April 2022), 103026. <https://doi.org/10.1016/j.seta.2023.103026>
- Bajaj, M., & Singh, A. K. (2020). Grid integrated renewable DG systems: A review of power quality challenges and state-of-the-art mitigation techniques. *International Journal of Energy Research*, 44(1), 26–69. <https://doi.org/10.1002/er.4847>
- Boopathi, R., & Indragandhi, V. (2023). Control techniques for renewable energy integration with shunt active filter: a review. *International Journal of Ambient Energy*, 44(1), 424–441. <https://doi.org/10.1080/01430750.2022.2128413>
- Boudechiche, G., Sarra, M., Aissa, O., & Gaubert, J. P. (2021). An investigation of solar active power filter based on direct power control for voltage quality and energy transfer in grid-tied photovoltaic system under unbalanced and distorted conditions. *Journal of Engineering Research (Kuwait)*, 9(3), 168–188. <https://doi.org/10.36909/jer.v9i3B.9061>
- Dash, D. K., & Sadhu, P. K. (2023). A Review on the Use of Active Power Filter for Grid-Connected Renewable Energy Conversion Systems. *Processes*, 11(5), 1467. <https://doi.org/10.3390/pr11051467>
- Debdouche, N., Deffaf, B., Benbouhenni, H., Laid, Z., & Mosaad, M. I. (2023). Direct Power Control for Three-Level Multifunctional Voltage Source Inverter of PV Systems Using a Simplified Super-Twisting Algorithm. *Energies*, 16(10), 4103. <https://doi.org/10.3390/en16104103>
- Djazia, K., & Sarra, M. (2023). Improving the quality of energy using an active power filter with zero direct power command control related to a photovoltaic system connected to a network. *Electrical Engineering and Electromechanics*, 5, 20–25. <https://doi.org/10.20998/2074-272X.2023.5.03>
- Essoussi, B., Moutabir, A., Bensassi, B., Ouchatti, A., Zahraoui, Y., & Benazza, B. (2023). Power Quality Improvement using a New DPC Switching Table for a Three-Phase SAPF. *International Journal of Robotics and Control Systems*, 3(3), 510–529. <https://doi.org/10.31763/ijrcs.v3i3.1042>
- Freitas, S., Oliveira, L. C., Oliveira, P., Exposto, B., Pinto, J. G., & Afonso, J. L. (2023). New Topology of a Hybrid, Three-Phase, Four-Wire Shunt Active Power Filter. *Energies*, 16(3). <https://doi.org/10.3390/en16031384>
- Imam, A. A., Sreerama Kumar, R., & Al-Turki, Y. A. (2020). Modeling and simulation of a pi controlled shunt active power filter for power quality enhancement based on p-q theory. *Electronics (Switzerland)*, 9(4), 637. <https://doi.org/10.3390/electronics9040637>
- Lumbreras, D., Gálvez, E., Collado, A., & Zaragoza, J. (2020). Trends in power quality, harmonic mitigation and standards for light and heavy industries: A review. *Energies*, 13(21), 1–24. <https://doi.org/10.3390/en13215792>
- Obaideen, K., Olabi, A. G., Al Swailmeen, Y., Shehata, N., Abdelkareem, M. A., Alami, A. H., Rodriguez, C., & Sayed, E. T. (2023). Solar Energy: Applications, Trends Analysis, Bibliometric Analysis and Research Contribution to Sustainable Development Goals (SDGs). *Sustainability (Switzerland)*, 15(2). <https://doi.org/10.3390/su15021418>
- Rajesh Garikapati, S. Ramesh Kumar, & N. Karthik. (2023). ANFIS Controlled MMC-UPQC to Mitigate Power Quality Problems in Solar PV Integrated Power System. *Journal of Advanced Research in Applied Sciences and Engineering Technology*, 36(1), 102–130.

<https://doi.org/10.37934/araset.36.1.102130>

Rath, A., & Srungavarapu, G. (2023). An Advanced Shunt Active Power Filter (SAPF) for Non-ideal Grid Using Predictive DPC. *IETE Technical Review (Institution of Electronics and Telecommunication Engineers, India)*, 40(4), 521–534. <https://doi.org/10.1080/02564602.2022.2127946>

Reguieg, Z., Bouyakoub, I., & Mehedi, F. (2024). Optimizing power quality in interconnected renewable energy systems: series active power filter integration for harmonic reduction and enhanced performance. *Electrical Engineering*.

Reguieg, Z., Bouyakoub, I., Mehedi, F., & Bouhadji, F. (2024a). Enhancing Electrical Grid Stability Through Power Quality Optimization via PV-PO-UPQC: An Integrated Approach. *2024 2nd International Conference on Electrical Engineering and Automatic Control (ICEEAC)*, 1–7.

Reguieg, Z., Bouyakoub, I., Mehedi, F., & Bouhadji, F. (2024b). Optimizing Power Quality : Simulation of UPQC Integrated PV with Comprehensive Reliability and Performance Analysis. *International Journal Of Smart Grid*, 8(1), 47–52.

Sahoo, B., Alhaider, M. M., & Rout, P. K. (2023). Power quality and stability improvement of microgrid through shunt active filter control application: An overview. *Renewable Energy Focus* , 44, 139–173. <https://doi.org/10.1016/j.ref.2022.12.006>

Sen, D., Kumar, S., Saha, T. K., & Dey, J. (2023). Active Power Control of DPC Based Operation of Three Phase Inverter Under Stand-Alone Mode. *Electric Power Components and Systems*, 51(3), 307–318. <https://doi.org/10.1080/15325008.2022.2148776>

Shi, L., & Jin, S. (2023). Direct torque control and space vector modulation-based direct torque control of brushless doubly-fed reluctance machines. *IET Electric Power Applications*, 17(8), 1069–1080. <https://doi.org/10.1049/elp2.12324>

Szromba, A. (2023). Improving the Efficiency of the Shunt Active Power Filter Acting with the Use of the Hysteresis Current Control Technique. *Energies*, 16(10), 4080. <https://doi.org/10.3390/en16104080>

Taghvaie, A., Warnakulasuriya, T., Kumar, D., Zare, F., Sharma, R., & Vilathgamuwa, D. M. (2023). A Comprehensive Review of Harmonic Issues and Estimation Techniques in Power System Networks Based on Traditional and Artificial Intelligence/Machine Learning. *IEEE Access*, 11(March), 31417–31442. <https://doi.org/10.1109/ACCESS.2023.3260768>